

OPEN

Quantitative Study of Vertebral Body and Paravertebral Muscle Degeneration Based on Dual-Energy Computed Tomography: Correlation With Bone Mineral Density

Zhenghua Liu, MM,* Yuting Zhang, MM,* Dageng Huang, MD,† Xiaowen Ma, MD,*
Yaqing Duan, MM,* and Yonghong Jiang, MD*

Objectives: This study aimed to quantify the degeneration of the vertebral body and paravertebral muscles using dual-energy computed tomography (DECT) and study its relationship with osteoporosis.

Methods: A total of 130 patients with chronic low back pain were included in this study, and DECT scanning of the lumbar region was undertaken prospectively. By placing a standard quantitative computed tomography corrected phantom under the waist during the DECT procedure, bone mineral density (BMD) and the following quantitative parameters were obtained: calcium density (CaD), vertebral fat fraction (VFF), psoas major area, psoas major fat fraction, erector spinalis area, and erector spinalis fat fraction (ESFF). Independent sample *t* test and 1-way analysis of variance were used between different age-BMD groups. Pearson test was applied to determine correlations for all measurements, and a mathematical model of BMD was established through regression analysis.

Results: Calcium density, VFF, psoas major area, psoas major fat fraction, erector spinalis area, and ESFF were significantly different among the age-BMD groups ($P < 0.05$), and BMD was significantly correlated with these parameters ($P < 0.05$). Calcium density, VFF, and ESFF were included in the BMD regression equation: $BMD = 69.062 + 11.637 \times CaD - 1.018 \times VFF - 0.726 \times ESFF$ ($R^2 = 0.860$, $F = 125.979$, $P < 0.001$).

Conclusions: Degeneration of the vertebral body and paravertebral muscles can be quantitatively analyzed using DECT, and CaD, VFF, and ESFF were independent influencing factors of BMD.

Key Words: bone mineral density, paravertebral muscle, fat infiltration, dual-energy computed tomography

(*J Comput Assist Tomogr* 2023;47: 86–92)

Osteoporosis (OP) is an increasingly serious problem in an aging society, mainly manifested by the degradation of bone microstructure and bone mineral density (BMD).¹ Recent studies have shown that bone and skeletal muscle, as common functional

units, participate in the pathological process of OP.^{2,3} Reduced mechanical loading generated by skeletal muscle is an important cause of bone mineral loss,⁴ and appropriate mechanical loading can delay or reverse the decline in aging of bone and skeletal muscle.^{5,6}

The decline in muscle strength is associated with structural changes, such as atrophy and fat infiltration, mainly in the form of a decrease in muscle volume (or cross-sectional area [CSA]) and an increase in muscle fat fraction (FF).^{7,8} Age-related degeneration of vertebral cancellous bone includes loss of BMD and morphological changes, including thinning of trabeculae and increase in intertrabecular spacing,⁹ which is filled by bone marrow adipose tissue (BMAT).¹⁰ Imaging techniques allow us to perform noninvasive quantitative studies of muscle and bone degeneration.

In the study of Fischer et al,¹¹ multiple imaging modalities were used to quantify muscle fat infiltration (MFI) in patients with lower back pain, arguing that dual-echo and multi-echo magnetic resonance imaging allows for rapid and accurate measurement of muscle fat content. In the studies of Zhao et al¹² and Pacicco et al,¹³ magnetic resonance imaging was used to assess muscle size and FF, and the results showed that muscle FF and CSA correlated with age and MFI resulted in lower lumbar spine BMD. The study of Sollmann et al¹⁴ concluded that there was also a significant correlation between vertebral body BMAT content and fat infiltration of the paravertebral muscles. In the aforementioned studies, the effect of vertebral and paravertebral muscle degeneration as a common mechanism of BMD has not been reported.

As a new quantitative method, dual-energy computed tomography (DECT) can quantify specific substances (calcium, fat, etc) with multimodal and multiparametric analysis¹⁵ and has shown great potential in quantitative studies of the musculoskeletal system.^{16–18} In this study, we aimed to quantify vertebral calcium density (CaD), BMAT, and paravertebral muscle CSA and FF in patients with different degrees of OP using DECT, to study their correlation with BMD, and to explore the relationship between vertebral body and paravertebral muscle degeneration and OP.

MATERIALS AND METHODS

Study Design

This study was conducted in accordance with the Declaration of Helsinki (as revised in 2013) and adopted a prospective design, which was approved by the Ethics Committee of our hospital (number 201902068). After obtaining informed consent of each participant, DECT scanning of the lumbar regions was performed from March 2019 to July 2021 in patients with chronic low back pain. The subjects were randomly selected, and then the scans were deemed necessary and advised by the spinal surgeons at our facility. The inclusion criteria were as follows: (1) 18 years or older and (2) signed informed consent. The exclusion criteria were as follows: (1) scoliosis, (2) after lumbar surgery, (3) lumbar

From the Departments of *Radiology, and †Spinal Surgery, Honghui Hospital Affiliated Xi'an Jiaotong University, Xi'an, China.

Received for publication May 30, 2022; accepted August 19, 2022.

Correspondence to: Dageng Huang, MD, Department of Spinal Surgery, Honghui Hospital Affiliated Xi'an Jiaotong University, No. 555, Youyi East Rd, Xi'an 710054, China (e-mail: hdgrichard@sina.com); or Yonghong Jiang, MD, Department of Radiology, Honghui Hospital Affiliated Xi'an Jiaotong University, No. 555, Youyi East Rd, Xi'an 710054, China (e-mail: 526017009@qq.com).

This work was supported by Shaanxi Provincial Key R & D Program (2021SF-240) and Shaanxi Provincial Key R & D Program (2020GXLH-Y-027). The funders had no role in study design, data collection and analysis, decision to publish, or preparation of the manuscript.

The authors declare no conflict of interest.

Copyright © 2022 The Author(s). Published by Wolters Kluwer Health, Inc. This is an open-access article distributed under the terms of the Creative Commons Attribution-Non Commercial-No Derivatives License 4.0 (CCBY-NC-ND), where it is permissible to download and share the work provided it is properly cited. The work cannot be changed in any way or used commercially without permission from the journal.

DOI: 10.1097/RCT.0000000000001388

fracture and bone destruction, (4) alcohol consumption of more than 50 mL per day, (5) taking adrenocortical hormone, and (6) chronic diseases such as chronic malnutrition and hyperthyroidism. By placing a standard quantitative computed tomography (QCT) corrected phantom (QCT Pro v5.0; Mindways, Austin, TX) under the waist during the DECT procedure, we obtained DECT parameters and QCT-based BMD concurrently.

DECT Scanning

Dual-energy computed tomography examinations relied on a second-generation 128-section dual-source unit operating in the dual-energy mode (Somatom Definition Flash; Siemens Healthineers, Erlangen, Germany). The settings of both x-ray tubes were constant (tube A: 80 kV, 250 mAs; tube B: 140 kV with Sn filter, 97 mAs). Other scanning parameters were set as follows: pitch, 0.6; collimation width, 32 × 0.6 mm; rotation time, 500 ms; field of view, 500 mm × 500 mm. The scanning range was extended from the 12th thoracic vertebra to the first sacral vertebra. Images were reconstructed using a kernel of I30f, 1-mm section thickness, and 0.75-mm increment. All radiation doses received by the patients were recorded upon completion.

Quantitation of Vertebral and Paravertebral Muscle

Quantitative measurements of the vertebrae and paravertebral muscles were performed based on the virtual noncontrast function module of the liver using dual-energy analytic software (Syngo. using VB10; Siemens Healthcare, Erlangen, Germany). In the configuration file under 80 kV/Sn140 kV tube voltage, the default value of soft tissue was 55 Hounsfield units (HU) and 51 HU, fat value was -110 HU and -87 HU, and iodine slope to 1.71 was modified.¹⁹

All vertebral and paravertebral muscle measurements were independently performed by 2 doctors with more than 8 years of experience in musculoskeletal radiology. The following quantitative parameters were measured on the axial images at the level of the third lumbar transverse process, including CaD, vertebral fat fraction (VFF), psoas major area (PMA) and psoas major fat fraction (PMFF), erector spinalis area (ESA), and erector spinalis fat fraction (ESFF), and the detailed measurement and calculation method are shown in Figure 1. The erector spinalis complex is composed of the iliocostalis, longissimus, and spinotransverse muscles (predominantly the multifidus) from the outside to the

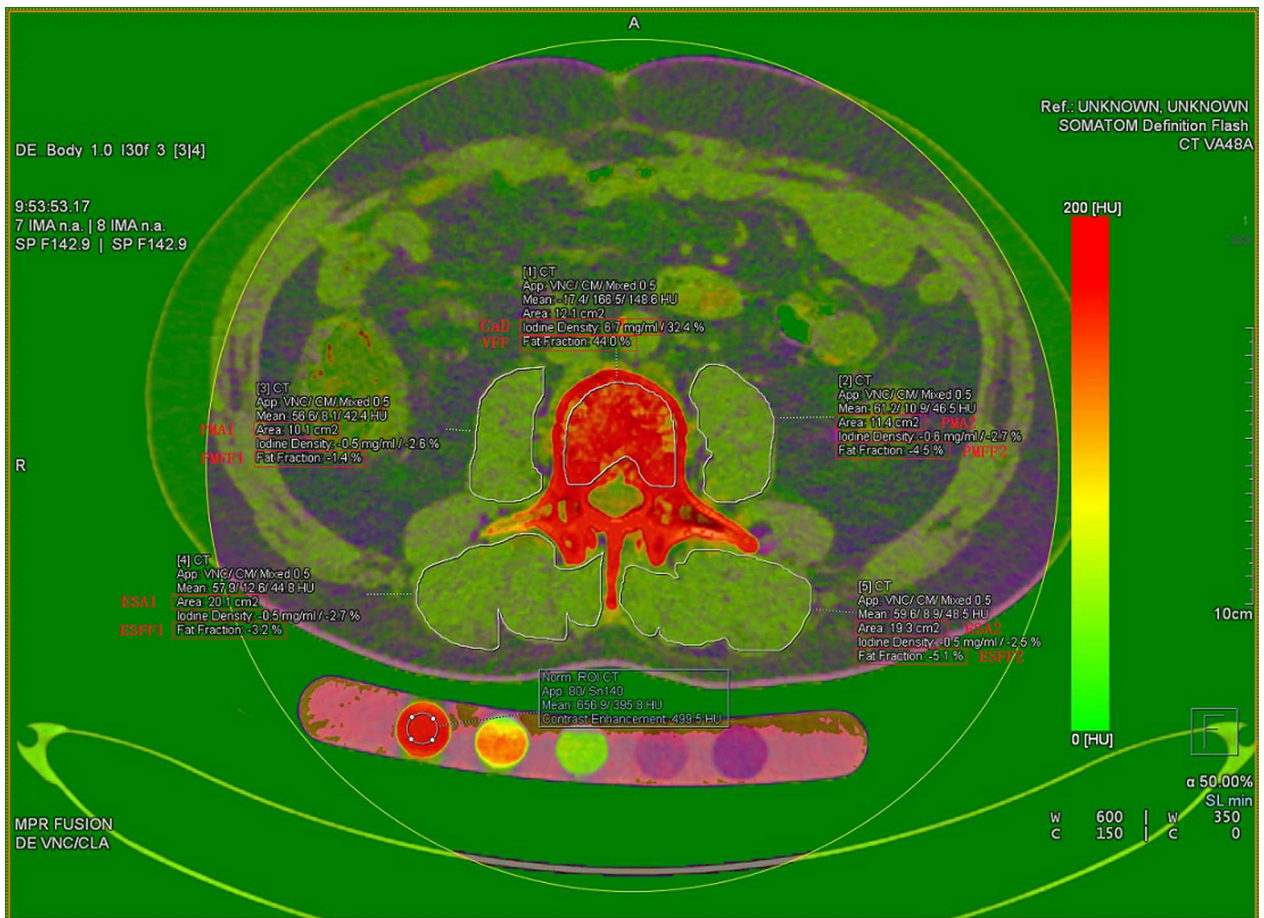


FIGURE 1. Measurement of quantitative parameters of vertebral body and paravertebral muscle. The CaD and VFF were measured by drawing a region of interest along the medial edge of the bone cortex of third lumbar vertebral body, avoiding the inner edge of the bone cortex and the osteosclerosis area around the vertebral vein groove. The muscle along the edges of psoas major and erector spinalis and the CSA and FF of paravertebral muscle were measured. The area and FF of bilateral psoas major muscle were recorded as PMA1, PMFF1, PMA2 and PMFF2, and the area and FF of bilateral erector spinalis muscle were recorded as ESA1, ESFF2, ESA1, and ESFF2, respectively. PMA = (PMA + PMA2)/2; PMFF = (PMFF1 + PMFF2)/2; ESA = (ESA1 + ESA2)/2; ESFF = (ESFF1 + ESFF2)/2.

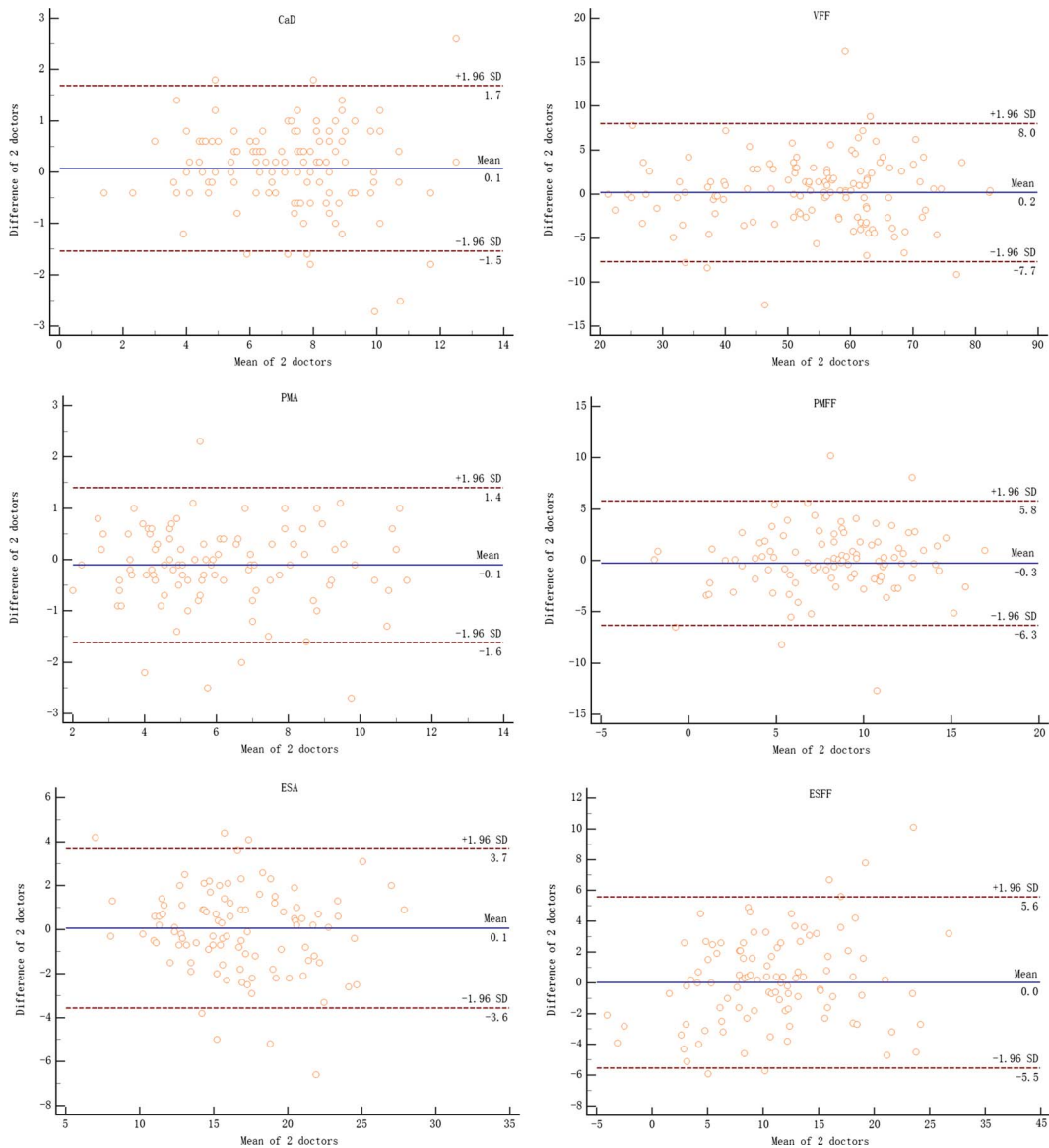


FIGURE 2. Bland-Altman analysis of 2 readers.

TABLE 1. Comparison of Age, BMI, and Quantitative Parameters (N = 130)

	Group A (n = 22)	Group B (n = 31)	Group C (n = 32)	Group D (n = 45)	F	P
Age, y	34.45 ± 5.59	52.74 ± 4.34	57.47 ± 6.34	62.24 ± 8.49	88.561	<0.001
BMI, kg/m ²	24.11 ± 3.26	25.51 ± 3.57	23.37 ± 3.95	24.03 ± 3.21	1.433	0.065
BMD, mg/cm ³	146.02 ± 18.19	136.33 ± 10.98	97.42 ± 10.72	51.64 ± 17.9	286.841	<0.001
CaD, mg/cm ³	9.27 ± 1.41	8.86 ± 1.5	7.23 ± 0.97	5.08 ± 1.36	73.320	<0.001
VFF, %	37.92 ± 8.33	38.53 ± 7.66	53.57 ± 7.63	57.4 ± 8.4	51.266	<0.001
PMA, cm ²	8.5 ± 2.42	6.4 ± 2.17	6.28 ± 1.92	5.12 ± 1.83	13.536	<0.001
PMFF, %	2.31 ± 3.16	5.76 ± 2.53	8.64 ± 2.97	9.83 ± 3.49	33.486	<0.001
ESA, cm ²	19.79 ± 4.9	16.76 ± 4.55	17.78 ± 3.34	15.11 ± 3.75	7.072	<0.001
ESFF, %	2.64 ± 4.05	9.64 ± 3.86	9.67 ± 3.42	14.04 ± 6.31	27.912	<0.001

Group A, young normal BMD group; group B, middle-aged and elderly normal BMD group; group C, osteopenia group; group D, OP group; BMI, body mass index.

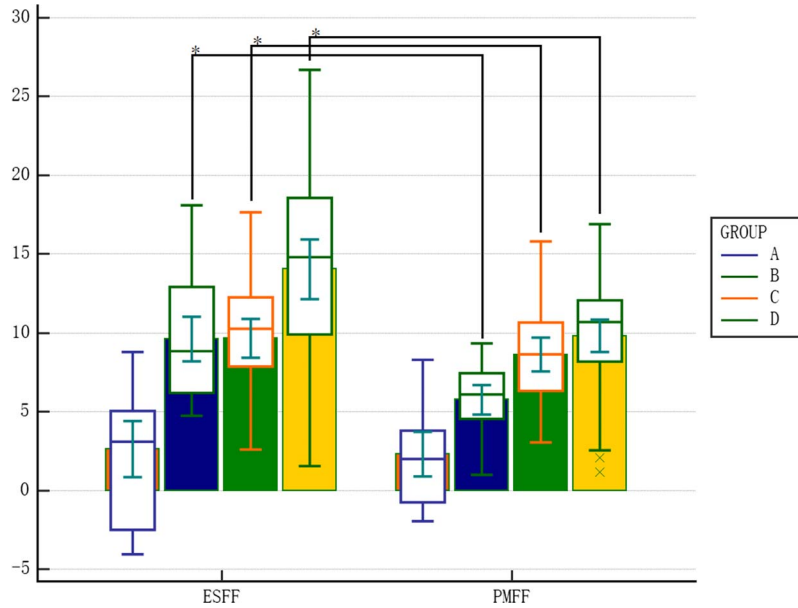


FIGURE 3. Psoas major fat fraction and ESFF in different age-BMD groups. **P* < 0.05; Group A, young normal group; group B, middle-aged and elderly normal group; group C, osteopenia group; and group D, OP group.

inside, and the region of interest was manually defined along the edge of the muscle.^{20,21}

BMD Measurement and Grouping

Dual-energy computed tomography data of mixed ratio (0.5) were imported to the QCT software (QCT Pro v5.0; Mindways) application, the BMDs of the first and second lumbar vertebrae were measured, and the mean value was taken as the final BMD value.²²

According to age and BMD, patients were divided into 4 groups: young normal BMD group (group A, younger than 45 years and BMD >120 mg/cm³), middle-aged and elderly normal BMD group (group B, 45 years or older and BMD >120 mg/cm³), osteopenia group (group C, 120 mg/cm³ ≥ BMD > 80 mg/cm³), and OP group (group D, BMD ≤80 mg/cm³).¹

Statistical Analysis

All computations were powered by MedCalc (version 19.0; MedCalc Software, Ostend, Belgium) and expressed as the mean ± SD. Consistency analyses for the measurements of the 2 readers were performed using the intraclass correlation coefficient. Variables were tested for normality of distribution using the Shapiro-Wilk test. Differences between groups were deter-

mined using the independent samples *t* test and 1-way analysis of variance. The Pearson test was used to determine the correlation between all measurements, and a mathematical model of BMD was established using multiple linear regression analysis. The significance for all tests was set at *P* value <0.05.

RESULTS

General Information

A total of 130 patients were included in this study. Of them, 52 were males and 78 were females, aged from 25 to 88 years, with an average age of 54.10 ± 11.66 years. The volume computed tomography (CT) dose index was 9.53 mGy, and the average dose-length product was 285.36 ± 37.56 mGy·cm, and the mean ± SD radiation dose was 3.99 ± 0.53 mSv.

Consistency Analysis

The CaD, VFF, PMA, PMFF, ESA, and ESFF values measured by the 2 doctors were in good agreement (intraclass correlation coefficient values were 0.929, 0.907, 0.946, 0.858, 0.914, and 0.899, respectively). The corresponding Bland-Altman plots are

TABLE 2. Correlation Analysis of Quantitative Parameters

Variables	CaD, mg/cm ³	VFF, %	PMA, cm ²	PMFF, %	ESA, cm ²	ESFF, %
BMD, mg/cm ³	0.880*	-0.756*	0.364*	-0.520†	0.313*	-0.671*
CaD, mg/cm ³		-0.630*	0.276*	-0.518*	0.222†	-0.496*
VFF, %			-0.285*	0.596*	-0.260*	0.384*
PMA, cm ²				-0.421†	0.659*	-0.543*
PMFF, %					-0.379†	0.619†
ESA, cm ²						-0.428*

**P* < 0.01.

†*P* < 0.05.

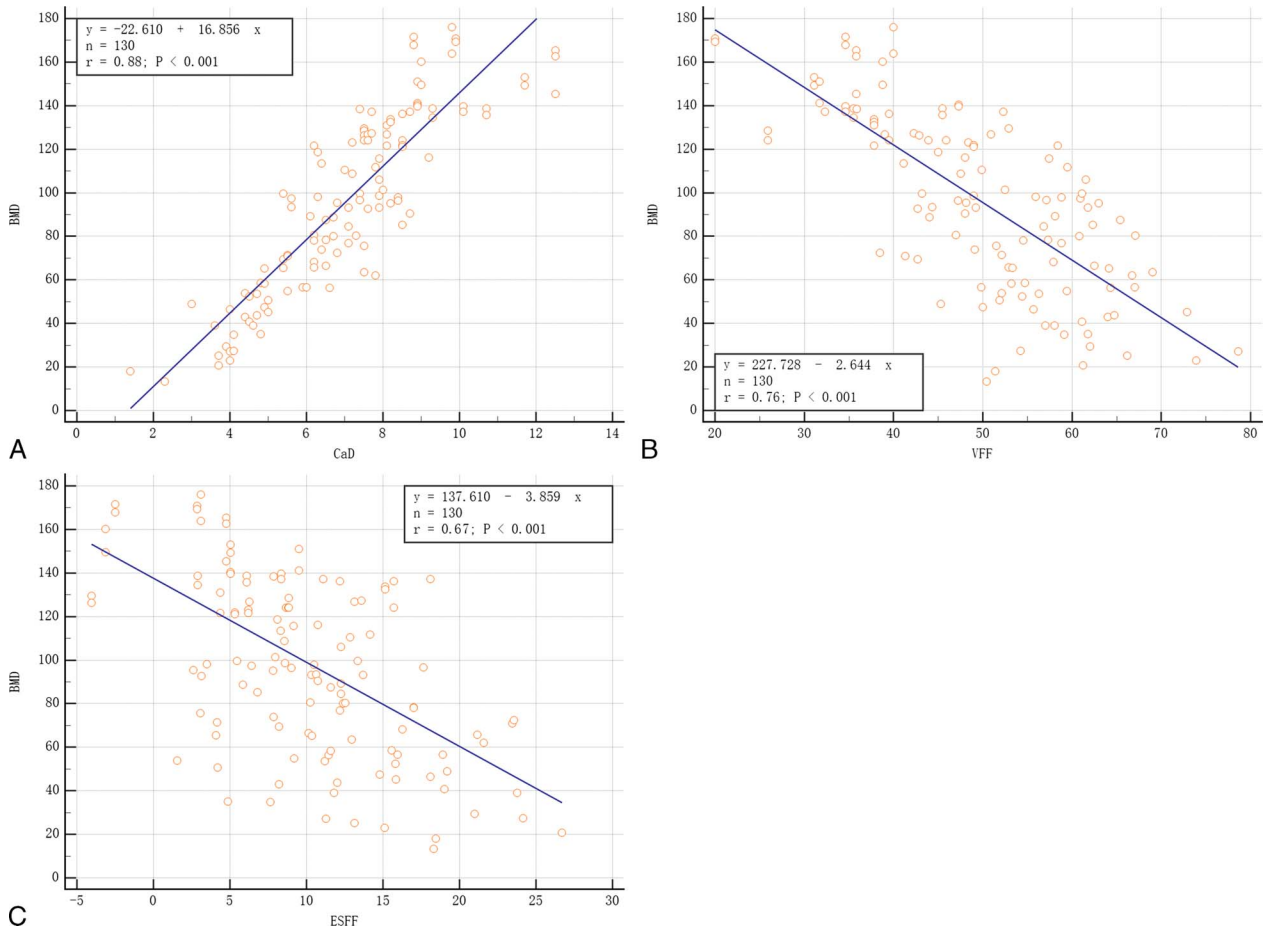


FIGURE 4. Linear correlation of CAD, VFF, ESFF, and regression predicted values with BMD.

shown in Figure 2, which indicate a reliable agreement between the observers.

Grouping

The age, body mass index, and quantitative parameters of DECT in the different groups are shown in Table 1. One-way analysis of variance showed that the CaD, VFF, PMA, PMFF, ESA, and ESFF were statistically different among the different age groups (F values were 73.320, 51.266, 13.536, 33.486, 7.072, and 27.912, respectively; all $P < 0.05$). An independent sample t test showed that there were significant differences between PMFF and ESFF in groups B, C, and D ($t = 4.681, P < 0.001; t = 1.286, P = 0.023; t = 3.917, P < 0.001$), but no significant difference was observed in group A ($t = 0.301, P = 0.0.765$) (Fig. 3).

Correlation and Regression Analysis

Bone mineral density was significantly correlated with all DECT parameters, including CaD, VFF, PMA, PMFF, ESA, and ESFF. Meanwhile, the CaD and VFF of the vertebrae were significantly correlated with the PMA, PMFF, ESA, and ESFF of the paravertebral muscles. All the correlation coefficients are listed in Table 2.

Multiple linear regression analysis showed that the CaD, VFF, and ESFF were ultimately included in the regression equation for BMD. The linear correlations between CAD, VFF, ESFF, standard regression predicted values, and BMD are shown in

Figure 4. The regression equation was expressed as $BMD = 69.062 + 11.637 \times CaD - 1.018 \times VFF - 0.726 \times ESFF$, and the regression model was statistically significant ($F = 125.979, P < 0.001$). The determinant coefficient was 0.860, and the partial regression coefficients (β) and standardization coefficient (β) of all independent variables are shown in Table 3.

DISCUSSION

Bone and muscle are the functional units that interact with each other. Muscle atrophy, decreased muscle strength, and decreased muscle function can accelerate the resorption of cortical bone, reduce the number and thinning of trabeculae in cancellous bone, and decrease BMD.² Changes in bone structure, such as spinal degeneration and scoliosis, can also lead to imbalances in the volume and MFI of paravertebral muscles.^{23,24} Our study showed that BMD and CaD of the lumbar vertebra significantly correlated with CSA and MFI of the paravertebral muscle, which is consistent with the aforementioned view and reflects the relationship between bone mineral loss of the vertebral body and degeneration of the paravertebral muscles. Multiple linear regression analysis showed that CaD was the most important positive factor affecting BMD, accounting for approximately 61%; VFF and ESFF were negative factors affecting BMD, accounting for 29% and 10%, respectively.

The synergistic effect of bone and muscle degeneration was also reflected in the association between BMAT and MFI. Bone

TABLE 3. Multivariate Linear Regression Analysis of BMD

Variables	B	SE	β	t	P
(Constant)	69.062	15.698	—	4.399	<0.001
CaD	11.637	0.894	0.607	13.017	<0.001
VFF	-1.018	0.168	-0.291	-6.066	<0.001
PMA	0.271	0.867	0.015	0.312	0.756
PMFF	-0.487	0.502	-0.048	-0.969	0.335
ESA	0.274	0.432	0.029	0.634	0.527
ESFF	-0.726	0.330	-0.107	-2.200	0.030

marrow adipocytes can play a role in systemic endoenvironmental homeostasis, including skeletal muscle homeostasis, through targeted endocrine action.²⁵ This was confirmed by the significant correlation of the VFF with the PMFF and ESFF in this study.

Notably, in the young normal group, there was no significant difference in FF between the psoas major and erector spinae, but with age and loss of BMD, FF in the erector spinae was significantly higher than in the psoas major, suggesting that fat infiltration in the psoas major and erector spinae was not synchronized, which is similar to the study by Lee et al.²⁶ We speculate that this may be related to the different mechanisms by which the psoas major and erector spinae muscles maintain mechanical properties of the spine. Contraction of the psoas major is associated with lower limb and lateral movements of the spine, whereas the erector spinae is subjected to more tension in the longitudinal direction during spinal activity and is more sensitive to biomechanical changes caused by spinal degeneration and BMD loss.

In addition, some studies have pointed out that the degree of fatty infiltration of the erector spinae varies at different intervertebral levels, especially in the lumbosacral region.^{26,27} In the study by Lee et al,²⁶ the data showed that the CSA and FF values of the paravertebral muscle at the L3 and L4 intervertebral disc level were relatively close to the mean values of all lumbar vertebral levels. In the present study, we considered L3 transverse process to be an appropriate level of observation. It was located in the middle of the vertebrae, which facilitated us to perform vertebral body and paravertebral muscle measurements in the same cross-section; as well as, it also takes into account the average of paravertebral muscle measurements at different lumbar levels.

Dual-energy computed tomography is a reliable method for quantifying the degree of fat infiltration in bones and muscles,^{17,18,28} but its biggest drawback is the use of ionizing radiation. With the development of several generations of DECT technology, the radiation dose has significantly reduced,²⁹ and the volume CT dose index of patients in this study was even lower than that of single-source CT abdominal scanning.³⁰ Also, opportunistic examinations were possible because OP evaluations were performed at the same time as the lumbar spine scans, which reduced the radiation dose specifically for bone densitometry.

This study has the following limitations. Manual outlining of the paravertebral muscles has some errors, and learning-based automatic segmentation techniques may be a better option,³¹ which requires a special software. In addition, paravertebral muscle volume is a better parameter for quantification compared with CSA at a single cross-section level, and it is recommended for investigation in future studies.

In conclusion, the degeneration of vertebrae and paravertebral muscles can be quantitatively analyzed by DECT, and CaD, VFF, and ESFF are independent influencing factors of BMD. Fatty infiltration in both bone marrow and paravertebral muscles plays an important role in the progression of OP.

ACKNOWLEDGMENT

The authors would like to express their sincere thanks to Yali Zhao, Jiangtao Kong, and Kai Liang, for their help regarding the patient treatment and DECT scanning.

REFERENCES

1. Ward RJ, Roberts CC, Bencardino JT, et al. ACR appropriateness criteria osteoporosis and bone mineral density. *J Am Coll Radiol.* 2017; 14(5S):S189–S202.
2. Ma HT, Griffith JF, Xu L, et al. The functional muscle-bone unit in subjects of varying BMD. *Osteoporos Int.* 2014;25:999–1004.
3. Grote C, Reinhardt D, Zhang M, et al. Regulatory mechanisms and clinical manifestations of musculoskeletal aging. *J Orthop Res.* 2019;37: 1475–1488.
4. Klein-Nulend J, Bakker AD, Bacabac RG, et al. Mechanosensation and transduction in osteocytes. *Bone.* 2013;54:182–190.
5. Kim JS, Jeon J, An JJ, et al. Interval running training improves age-related skeletal muscle wasting and bone loss: experiments with ovariectomized rats. *Exp Physiol.* 2019;104:691–703.
6. Hu S, Yang L, Wu C, et al. Regulation of Wnt signaling by physical exercise in the cell biological processes of the locomotor system. *Physiol Int.* 2019;106:1–20.
7. Engelke K, Museyko O, Wang L, et al. Quantitative analysis of skeletal muscle by computed tomography imaging—state of the art. *J Orthop Translat.* 2018;15:91–103.
8. Han G, Jiang Y, Zhang B, et al. Imaging evaluation of fat infiltration in paraspinal muscles on MRI: a systematic review with a focus on methodology. *Orthop Surg.* 2021;13:1141–1148.
9. Ferguson SJ, Steffen T. Biomechanics of the aging spine. *Eur Spine J.* 2003; 12(suppl 2):S97–S103.
10. Sebo ZL, Rendina-Ruedy E, Ables GP, et al. Bone marrow adiposity: basic and clinical implications. *Endocr Rev.* 2019;40:1187–1206.
11. Fischer MA, Nanz D, Shimakawa A, et al. Quantification of muscle fat in patients with low back pain: comparison of multi-echo MR imaging with single-voxel MR spectroscopy. *Radiology.* 2013;266:555–563.
12. Zhao Y, Huang M, Serrano Sosa M, et al. Fatty infiltration of paraspinal muscles is associated with bone mineral density of the lumbar spine. *Arch Osteoporos.* 2019;14:99.
13. Pacicco T, Ratner S, Xi Y, et al. Pelvic muscle size and myosteatosis: relationship with age, gender, and obesity. *Indian J Radiol Imaging.* 2019; 29:155–162.
14. Sollmann N, Dieckmeyer M, Schlaeger S, et al. Associations between lumbar vertebral bone marrow and paraspinal muscle fat compositions—an investigation by chemical shift encoding-based water-fat MRI. *Front Endocrinol (Lausanne).* 2018;9:563.
15. Cao Q, Shang S, Han X, et al. Evaluation on heterogeneity of fatty liver in rats: a multiparameter quantitative analysis by dual energy CT. *Acad Radiol.* 2019;26:e47–e55.
16. Molwitz I, Leiderer M, Özden C, et al. Dual-energy computed tomography for fat quantification in the liver and bone marrow: a literature review. *Rofo.* 2020;192:1137–1153.
17. Baillargeon AM, Baffour FI, Yu L, et al. Fat quantification of the rotator cuff musculature using dual-energy CT-A pilot study. *Eur J Radiol.* 2020; 130:109145.
18. Molwitz I, Leiderer M, McDonough R, et al. Skeletal muscle fat quantification by dual-energy computed tomography in comparison with 3T MR imaging. *Eur Radiol.* 2021;31:7529–7539.
19. Liu Z, Zhang Y, Liu Z, et al. Dual-energy computed tomography virtual noncalcium technique in diagnosing osteoporosis: correlation with quantitative computed tomography. *J Comput Assist Tomogr.* 2021;45: 452–457.

20. Crawford RJ, Cornwall J, Abbott R, et al. Manually defining regions of interest when quantifying paravertebral muscles fatty infiltration from axial magnetic resonance imaging: a proposed method for the lumbar spine with anatomical cross-reference. *BMC Musculoskelet Disord.* 2017;18:25.
21. Griffith JF, Yeung DK, Antonio GE, et al. Vertebral marrow fat content and diffusion and perfusion indexes in women with varying bone density: MR evaluation. *Radiology.* 2006;241:831–838.
22. Morse LR, Biering-Soerensen F, Carbone LD, et al. Bone mineral density testing in spinal cord injury: 2019 ISCD official position. *J Clin Densitom.* 2019;22:554–566.
23. Xie D, Zhang J, Ding W, et al. Abnormal change of paravertebral muscle in adult degenerative scoliosis and its association with bony structural parameters. *Eur Spine J.* 2019;28:1626–1637.
24. Jiang J, Meng Y, Jin X, et al. Volumetric and fatty infiltration imbalance of deep paravertebral muscles in adolescent idiopathic scoliosis. *Med Sci Monit.* 2017;23:2089–2095.
25. de Paula FJA, Rosen C. Marrow adipocytes: origin, structure, and function. *Annu Rev Physiol.* 2020;82:461–484.
26. Lee SH, Park SW, Kim YB, et al. The fatty degeneration of lumbar paraspinal muscles on computed tomography scan according to age and disc level. *Spine J.* 2017;17:81–87.
27. Crawford RJ, Filli L, Elliott JM, et al. Age- and level-dependence of fatty infiltration in lumbar paravertebral muscles of healthy volunteers. *AJNR Am J Neuroradiol.* 2016;37:742–748.
28. Bredella MA, Daley SM, Kalra MK, et al. Marrow adipose tissue quantification of the lumbar spine by using dual-energy CT and single-voxel (1)H MR spectroscopy: a feasibility study. *Radiology.* 2015;277:230–235.
29. John D, Athira R, Selvaraj S, et al. Does dual-energy abdominal computed tomography increase the radiation dose to patients: a prospective observational study. *Pol J Radiol.* 2021;86:e208–e216.
30. Schmidt D, Soderberg M, Nilsson M, et al. Evaluation of image quality and radiation dose of abdominal dual-energy CT. *Acta Radiol.* 2018;59:845–852.
31. Kamiya N, Li J, Kume M, et al. Fully automatic segmentation of paraspinal muscles from 3D torso CT images via multi-scale iterative random forest classifications. *Int J Comput Assist Radiol Surg.* 2018;13:1697–1706.